An innovative way to enhance the high temperature properties of alkali activated cement mortars prepared by using glass powder as precursor

Binyu Zhang · Pingping He · Chi Sun Poon

Abstract This paper presents an innovative way of enhancing the residual strength and the dimensional stability after elevated temperature exposures for Alkali Activated Cement (AAC) mortar prepared with recycled glass materials as the principle precursor and fine aggregate. The reference AAC mixture was prepared with Glass Powder (GP) solely as the precursor material. A 28-day compressive strength of slightly over 10 MPa was attained but the samples experienced severe dimensional instability (expansion) after 2 h of exposure to 800 °C. To address this problem, 10% to 25% calcium aluminate cement (CAC) was used to replace the GP and the expansion was effectively controlled when the amount of CAC reached 15%. Also, significant strength increment was attained after the elevated temperature resistance test. The severe expansion of the reference mortar was attributed to the density reduction and volume expansion of the recycled glass materials at the elevated temperature and an extremely porous structure (porosity of over 50%) was resulted after the test. Meanwhile, for the CAC incorporated mixtures, the dehydration of sodium aluminum silicate hydrate at temperature ranging from 250–270 °C enabled sufficient space to accommodate the glass materials

expansion. The results show that with the incorporation of CAC, recycled glass dominated AAC mortars that contain higher than 80% total recycled glass materials can be fabricated. A residual strength increment of up to 450% can be obtained while maintaining the original dimension without expansion after the elevated temperature exposure.

Keywords Recycled glass cullet (GC) · Recycled glass powder (GP) · AAC mortar · Elevated temperature resistance · Dimensional stability

1 Introduction

In Hong Kong, a large quantity of waste glass materials ended up in the already filled up landfills daily, resulted from the limited land and the lack of glass bottle recycling factories. The recycling and reuse of the waste glass materials contributes to sustainable waste management and resources conservation. The use of glass waste in construction materials is considered an effective method to mitigate this solid waste issue. Recycled Glass Cullet (GC) have been used as an alternative aggregate to substitute natural fine aggregates such as river sand [1–3]. Also the use of GP derived from grinding the recycled GC is also gaining increasing attention [4–6]. The combined use of both recycled GC and recycled GP helps to

B. Zhang · P. He · C. S. Poon (✉)
Department of Civil and Environmental Engineering, The Hong Kong Polytechnic University, Hung Hom, Kowloon, Hong Kong
e-mail: cecspoon@polyu.edu.hk

maximize the recycling rate of this type of waste material.

Using as a fine aggregate, recycled GC was reported to have positive effects on the elevated temperature resistance capacity for both ordinary Portland cement (OPC) based materials [7, 8] and AAC based materials [9]. The possible use of GP as a pozzolanic material attracted much research interest. It has been demonstrated that recycled GP can be used for partially replace OPC to produce cement mortars or concrete [10–12]. Similar to other conventional supplementary cementitious materials, the incorporation of recycled GP was found effective for improving the durability properties [13] of cement based products, including reduced strength losses induced by elevated temperature exposures [14].

Recent research works reported that the use of waste GP to replace granulated blast furnace slag (GGBS) as a precursor material in the AAC system resulted in reduction in strength due to the lower reactivity of recycled glass materials compared to GGBS [9]. But another study showed that when the median particle size of recycled GP was reduced to 13 μm, the GP possessed a higher reactivity than metakaolin [4]. When further ground to a median size of about 5 μm, the recycled GP even possessed a higher reactivity than fly ash [15] in the AAC system as indicated by the strength development.

Despite of the fact that the recycled GP has been used in research studies as a supplementary cementitious material and a precursor respectively in OPC and AAC systems, limited work has reported the use of GP as the principal precursor in AAC mortars. It was concluded in a recent review paper that it is impossible to obtain desired mechanical properties with GP only as the precursor material [16]. Among all the previous studies regarding the recycling and reusing of waste glass materials in construction materials, the recycled GP was only considered as a supplementary component due to the strength loss resulted from the relatively low reactivity of the material [17]. However, in order to mitigate the solid waste problem effectively, investigations on the AAC mortars using GP as the principal or even sole precursor is of great importance.

It is well recognized that AAC based concrete has a better elevated temperature resistance capacity compared to OPC concrete [18]. However, previous studies were focused only on the mechanical properties which were indicated mostly by the residual compressive strength [9] or residual flexural strength ratios [19]. Few publications were found regarding the dimensional stability of AAC mortars after subjecting to the elevated temperature conditions. The dimensional stability issue would be more important for AAC using GP as common soda-lime glass's glass transition temperature is about 650 °C and the heated AAC mortars may be deformed after the high temperature exposure.

The hydration of calcium aluminate cement (CAC) has been studied previously, it was reported [20] that under room temperature conditions, the main hydrated products included $CaAl_2O_4 \cdot 10H_2O$ (CAH_{10}) and $Ca_2Al_2O_5 \cdot 8H_2O$ (C_2AH_8), out of which the CAH_{10} showed a higher stability. Whereas a recent study [21] suggested a precipitation sequence of hydrates in the order of CAH_{10} & C_2AH_x > Carbonated AFm > C3AH$_6$. The use of CAC in AAC mortars for properties improvement attracted attentions in recent years. Conventionally, the precursors in AAC paste are silico-aluminium rich materials [22, 23], though GP contains a considerable amount of SiO_2, there is only negligible aluminium in the material, and CAC could serve as an extra Al source. When extra aluminium sources were added into AAC systems, the Al could participate in the geopolymerization reaction to form cross-linking structures [24]. At the same time, depends on the alkalinity of the activator, CAC's hydration reaction took place and hydration products such as AH_3 and/or CAH_{10} [25] could be generated. In a previous study, CAC was added to GP based AAC mortars attempting to enhance the mechanical properties for GP based AAC mortars, three types of CAC was used as part of the precursor materials, and it was found out that CAC had a positive impact on strength development due to the promoted degree of reaction and improved sodium aluminosilicate (N-A-S–H) gel formation [26]. Incorporating CAC as a minor component in the AAC mortars to constitute < 25% of the precursor materials by mass enabled better performances in terms of alkali-silica reaction (ASR) induced expansion suppression and residual strength retaining after elevated temperature resistance test [27], and the optimal CAC dosage wasbetween 10 to 15% [28].

The objective of this study is to investigate the elevated temperature resistance capacity of AAC mortars using recycled GP solely as the precursor

and to develop an effective way to resolve the dimensional stability issue of the GP-only AAC mortar. Experimental works were designed to systematically investigate the effect of CAC on the elevated temperature resistance capacity of the GP-AAC mortar. Mechanical properties before and after the elevated temperature tests were evaluated and analysed. Microstructural tests were also conducted for better understanding of the mechanism.

2 Experimental program

2.1 Materials

2.1.1 Recycled GC

The recycled waste glass used in this study was provided by a local glass recycling factory, and the majority of which was sourced from crushed waste glass beverage bottles. The recycled GC comprised various coloured waste glass. Preliminary cleaning, drying and sieving was carried out before the GC was used. No pre-treatment other than the crushing and cleaning and sieving process was conducted for the GC, therefore the GC aggregate used in this study was angular in shape. The sieving analysis results of the GC is illustrated by Fig. 1.

2.1.2 Recycled GP and CAC

The recycled GP was prepared by grinding the prepared GC using a laboratory ball mill for 4 h. Previous research indicated GP possessed suitable reactivity to be used in AAC system when ground to a median particle size of about 50 μm [9]. In this study,
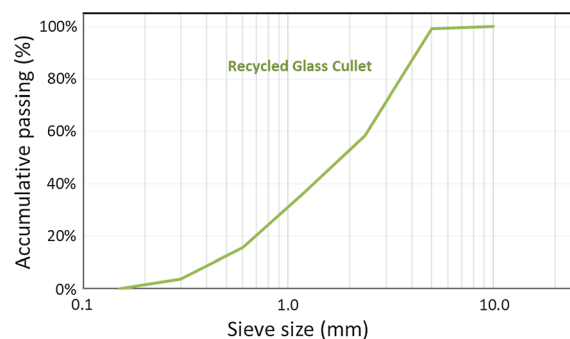
the ground mixed coloured GP was with a median particle size of about 38 μm. The other powder material, CAC, was sourced commercially.

The particle size analysis (PSA) was performed with a Laser Diffraction Particle Size Analyzer, (Malvern MASTERSIZER 3000E), and ethanol was used as the dispersant. The particle size analysis results of the GP and CAC are shown in Fig. 2. It can be seen from Fig. 2 that the particle size of the GP was slightly coarser than the CAC.

The chemical compositions of GP and CAC were determined by X-ray fluorescence (XRF) (*Rigaku Supermini200). The chemical compositions of the GP and CAC are listed in Table 1.

2.1.3 Activators

The activator used was prepared from a commercially available sodium silicate (water glass), and its effective total solid content was 36.9% (28.3% SiO_2 and 8.6% Na_2O by mass). Appropriate dosages of sodium hydroxide (NaOH, industrial grade) and water were added in order to obtain the desired activator solution. Activators with a fixed modulus MR (molar ratio of $SiO_2:Na_2O$) = 1.5 was prepared as the optimized MR [28]. The dosage of activator was represented by a/p as the ratio of total activators' equivalent solid content to the amount of precursor by mass. The activators were prepared 24 h before use.

2.2 Mix proportions

The AAC mixtures were designed based on a total precursor content of 1.0. A fixed dosage of activator to powder ratio a/p = 0.15 was used [28]. The total mass of precursors and the equivalent solid content of the
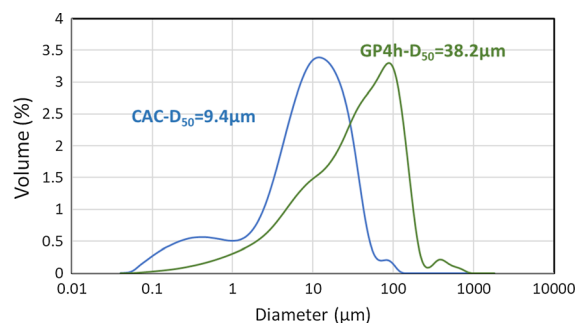

Fig. 1 Sieve analysis of mixed size recycled glass cullet

Fig. 2 Particle size distributions of recycled GP (ground 4 h) and CAC

Table 1 Chemical compositions of GP and CAC (wt.%)

	Na_2O	MgO	Al_2O_3	SiO_2	SO_4	K_2O	CaO	TiO_2	Cr_2O_3	MnO	Fe_2O_3
GP	12.74	1.25	0.73	73.50	–	0.69	10.48	0.09	0.12	0.01	0.38
CAC	–	0.24	57.03	2.65	0.32	0.21	38.76	–	–	–	0.65

activator was considered as the total binder. The amounts of aggregate, water and dosage of admixtures were calculated based on the relative mass of the total binder.

The reference mixture was prepared by using the GP only as the precursor and coded GP100. CAC was then gradually introduced to partially replace GP from 10 to 25% by mass. Recycled GC with size less than 3.55 mm was used as the fine aggregate. A fixed aggregate to binder ratio Agg/b of 2.0 was used for all mixtures, the aggregate ratio was set based on previous optimization by the authors [28], and a fixed water to binder ratio w/b of 0.30 were used in order to avoid bleeding for fresh mixed reference GP100 AAC mortar.

The detailed mix proportions are listed in Table 2.

In order to carry out the TGA, XRD and FTIR tests, separated mortar specimens were casted as shown in Table 3. Mono-sized GC was used to facilitate aggregate-paste separation to obtain the pure AAC paste before powder grinding.

2.3 Mixing, curing and testing

The activator solutions were prepared 24 h before casting to allow the cooling down of them to room temperature before use. The fresh AAC mixtures were prepared using a mechanical mortar mixer with a capacity of 5L/batch, and the total mixing time was controlled at 5 min.

For all the mixtures, cylindrical specimens sized Φ50mm*H50mm and Φ25mm*H20mm were casted and tested.

The specimens were demolded 24 h after casting and sealed in airtight plastic containers immediately. The containers were then stored in the laboratory with temperature 23 ± 5 °C for ambient temperature curing.

For all the specimens before and after exposure to the elevated temperatures, cylindrical specimens sized Φ50mm*H50mm were used for the compressive strength test. The test was conducted at a fixed loading rate 0.6 MPa/s in accordance with a modified standard teste method given by ASTM C109.

As for the elevated temperature resistance test, at the designed testing age, the specimens were placed into an electric furnace which was heated up at a rate of 2.5 °C/min from room temperature to 800 °C. The specimens were allowed to stay in the furnace at this temperature for 2 h. The post-high temperature exposure strength was then tested after the specimens were cooled down naturally to room temperature. The residual compressive strength was calculated for evaluation and analysis.

The diameter of the bottom side of the cylinders sized Φ25mm*H20mm were measured after the test to evaluate the dimensional stability of the specimens

Table 2 Mix proportions of AAC mortars (wt.%)

Mix code	Powder		Activator		GC	Water	Recycled glass materials content by mass		
	GP	CAC	MR	a/p	Agg/b	w/b	GP (%)	GC (%)	Total (%)
GP100	1.00	–	1.5	0.15	2.0	0.30	26.3	60.4	86.6
CAC10	0.90	0.10	1.5	0.15	2.0	0.30	23.6	60.4	84.0
CAC15	0.85	0.15	1.5	0.15	2.0	0.30	22.3	60.4	82.7
CAC20	0.80	0.20	1.5	0.15	2.0	0.30	21.0	60.4	81.4
CAC25	0.75	0.25	1.5	0.15	2.0	0.30	19.7	60.4	80.1

Table 3 Mix proportions of mortar samples prepared for TGA, XRD and FTIR tests (wt.%)

Mix code	Powder		Activator		GC (2.36–5 mm)	Water
	GP	CAC	MR	a/p	Agg/b	w/b
GP100-Mortar	1.00	–	1.5	0.15	2.0	0.30
CAC15-Mortar	0.85	0.15	1.5	0.15	2.0	0.30

which is indicated by the average expansion ratio of the cross-sectional area.

The microstructure examination was conducted by a set of Scanning Electron Microscopy-Backscattered-Electron (SEM-BSE) Imaging equipment (Tescan VEGA3). For the SEM-BSE test, after the specimens reached the designed curing age, two slices with a thickness of 5 mm ± 1 mm were cut from the small cylindrical specimens with sized Φ25mm. One slice was immersed immediately in ethanol to stop further reaction, the other slice was heated in the furnace together with the specimens sized Φ50mm*H50mm. After the high temperature exposure, the slice was also immersed in ethanol. Before the characterization, the ethanol was removed by drying at 60 ℃ for 48 h. The specimens were then casted into an epoxy resin (Buehler EpoThin 2 Epoxy Resin mixed with Buehler EpoThin 2 Epoxy Hardener) under vacuum conditions. Polishing was applied to obtain a flat and smooth surface (0.5 μm) for characterization by the SEM-BSE. Elemental characterization was performed at a fixed magnification of 100 times using Energy-dispersive X-ray spectroscopy (EDX). For porosity characterization, the specimens were examined at a fixed magnification of 200 times. An Image Analysis Software (Image-Pro) was employed to determine the porosity of the AAC specimens.

After the microstructure and elemental characterizations, the epoxy impregnated specimens were polished again for micro-hardness evaluation using a set of HVX-1000 digital micro hardness tester. For each sample, 40–80 measurements were recorded to plot the Vickers hardness distribution profiles.

Separately, powder samples were prepared for further test. For the 2 mixtures of mortars (GP100 and CAC15) listed in Table 3, both specimens before and after the elevated temperature resistance test (800 ℃ for 2 h) were collected, and after manually removing the GC aggregates, powder samples were ground from the remaining pastes and sieved to pass the 45 μm sieve for thermal gravimetric analysis (TGA), X-ray diffraction (XRD) and chemical functional group characterization via Fourier-transformed infrared spectroscopy (FTIR) tests.

The A set of Mettler Toledo TGA/DSC3+ was employed to perform the TGA test with the temperature of the furnace programmed to rise at a constant heating rate of 25 °C/min up to 900 °C under inert gas flow (N_2) at a constant rate of 50 mL/min. For XRD test, sample was acquired from the same batch used for TGA test. Before the test, the powder samples were placed under vacuum environment with temperature 60 °C for 48 h. A set of Rigaku SmartLab X-ray Diffractometer was used for the XRD test. The scanning range was 0–70 degrees. A set of PerkinElmer UATR two Spectrometer was used for the FTIR test, and the wavenumber used ranged from 2000 to 400 cm^{-1} with a resolution of 2 cm^{-1}.

A set of PerkinElmer UATR two FTIR Spectrometer was used for the FTIR test, the wavenumber started from 2000 to 400 cm^{-1} with resolution of 2 cm^{-1}.

3 Results and discussion

3.1 Mechanical properties

For the cylindrical specimens sized Φ50mm*H50mm, capping was applied with gypsum plaster before the compressive strength test to minimize the bias induced by uneven surfaces. The strength test results can be found in Fig. 3. The residual strength ratio was calculation in accordance with Eq. (1):

$$\text{Residual strength ratio} = \frac{\sigma - \text{After test (MPa)}}{\sigma - \text{Before test (MPa)}} \times 100\%$$
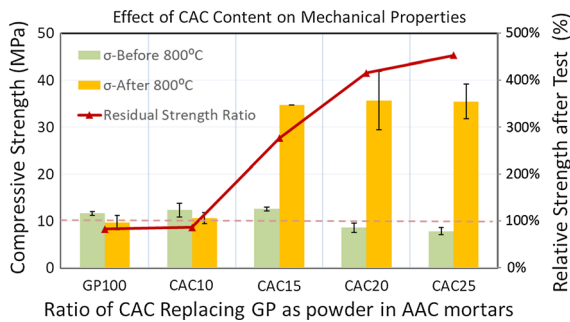
(1)

Fig. 3 Compressive strength of AAC mortars tested under room temperature, after subjected to the elevated temperature resistance test and the residual strength ratio calculated

As illustrated by Fig. 3, after 28-day curing under ambient temperature, the reference mixture GP100 exhibited a compressive strength of about 11 MPa, and the strength was relatively low compared to the conventional GGBS or fly ash based AAC mortars mainly due to the low reactivity of the recycled GP [17]. A similar strength value was reported in the recycled GP dominated geopolymer mortars [26]. With using 10% and 15% CAC to replace the recycled GP, slight strength increments were recorded. However, when the CAC content exceeded 20% as the total precursor, strength loss was detected, which was attributed to the zeolite formation when excessive CAC was added in the system [29].

For the strength values after the elevated temperature exposure, the reference mortar mixture and the AAC mortar prepared with 10% CAC both exhibited over 10% strength losses. However, as the CAC content was increased to 15%, significant strength increase was attained after the high temperature test. For the CAC15 mortar, the elevated temperature exposure led to a residual strength of about 35 MPa, which was 276% of the strength before the test. When the CAC content was further increased to 20% and 25% of the total powder content, a similar strength value to that of CAC15 was detected. The very high increase in residual strength ratios (415% and 453%) were partly due to the lower initial strength values of the mixtures before the high temperature exposure. This residual strength increment could be attributed to the reduced porosity and the enhanced microhardness of paste after exposure to elevated temperature. The details are discussed in the Sect. 3.3.

3.2 Dimensional stability

For the reference mixture GP100, significant expansion occurred as shown in Fig. 4a. But for the CAC incorporated specimens, instead of expansion, slight shrinkage occurred after the test when the CAC content reached 25% of the total precursor, as shown in Fig. 4b.

The cross-sectional area of the specimens before and after the high temperature tests were measured and the results are summarized in Fig. 5. The cross sectional area alternation ratio was calculation in accordance with Eq. (2):

Cross sectional area alternation ratio

$$= \frac{\text{Cross section area} - \text{After test } (\text{mm}^2)}{\text{Cross section area} - \text{Before test } (\text{mm}^2)} \times 100\%$$

(2)

The expansion was mainly due to the annealing of the un-reacted glass materials as the density of soda lime glass was reduced when the temperature was increased. The volume of the glass materials was increased and thus expansion occurred [30].

From the data summarized in Fig. 5 it can be seen that the incorporation of CAC was effective in controlling the dimensional stability of the specimens. The degree of expansion reduced as the dosage of CAC was increased gradually from 10 to 25% of the total precursor by mass. When the CAC content was increased to 15% of the total powder content, negligible dimensional change was detected after exposure to the elevated temperature. Further increasing the CAC content to 25% even induced slight shrinkage in the specimens. Therefore, three mixtures GP100, CAC15 and CAC25, representing the GP based AAC mortars exhibiting severe expansion, negligible change and slight shrinkage respectively, were selected for further investigations.

In this study, two major indexes were used for the elevated temperature resistance capacity evaluation: namely (i) the cross-section area change and (ii) residual compressive strength ratios, after the test. Correspondingly, microstructural tests were designed for mechanism investigations.
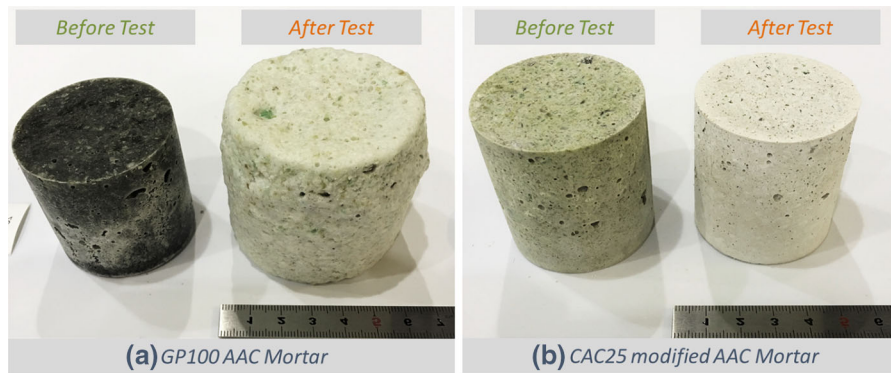
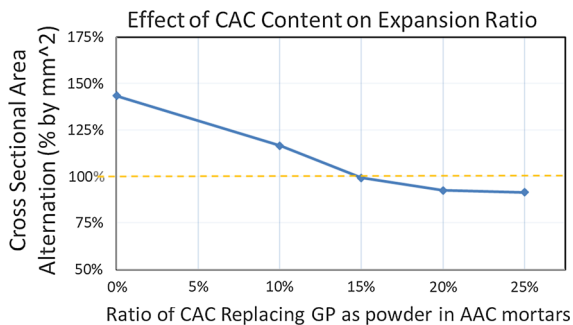Fig. 4 Cylindrical specimens before and after exposure to 800 °C

Fig. 5 Cross sectional area alternation ratios of cylindrical specimens after exposure to 800 °C

3.3 Microstructural test

3.3.1 SEM-BSE

The SEM-BSE images acquired for GP100, CAC15 and CAC25 mortars are shown in Fig. 6.

For the porosity quantification, the images of a fixed magnification of 200 times were used. The average porosity values determined by the image analysis software-Image Pro before and after the elevated temperature exposure are presented in Fig. 7.

As shown in Fig. 6, before the AAC mortars were subject to the elevated temperature conditions, clear boundaries could be detected between the GC aggregate and the AAC paste. While after the test, for GP100 mortar, the paste and aggregate fused and a large amount of pores were left. An extremely porous structure was resulted from the elevated temperature exposure. The average porosity reached 50.9%. The high porosity could be attributed to the annealing of the recycled glass materials. As the temperature was raised to above 550 °C, the density of the recycled

glass materials decreased [30], the volume expanded and the dimensional stability was significantly affected. While during the cooling down process, the recycled glass materials shrank as the density increased, consequently, a considerable amount of pores were left and the residual strength was impacted.

For CAC15 and CAC25 mortars, after the test, less distinctive boundaries between the GC aggregate and the AAC paste was formed as a result of GC annealing, indicating an improved bonding between the recycled GC and the matrix. According to the authors' previous study [31], recycled glass annealing accompanied with Si release into the AAC paste is pivotal for the bonding and residual strength enhancement. The dehydration of CAC hydration products left pores that might help to mitigate the expansion pressure generated from recycled glass annealing during high temperature exposure. Therefore, this may explain the improved dimensional stability of the AAC mortars prepared with the incorporating CAC after the high temperature exposure.

The reduction of porosity can also explain the strength enhancement after the high temperature exposure [32]. As shown in Fig. 7, for GP100 mortar, an obvious porosity increment was detected after the elevated temperature resistance test, however, for both CAC15 and CAC25 mortars, less porous structures were formed after the test. With 15% and 25% CAC incorporation, the porosity of the sample after the test were effectively reduced to 17.8% and 15.0%, respectively.
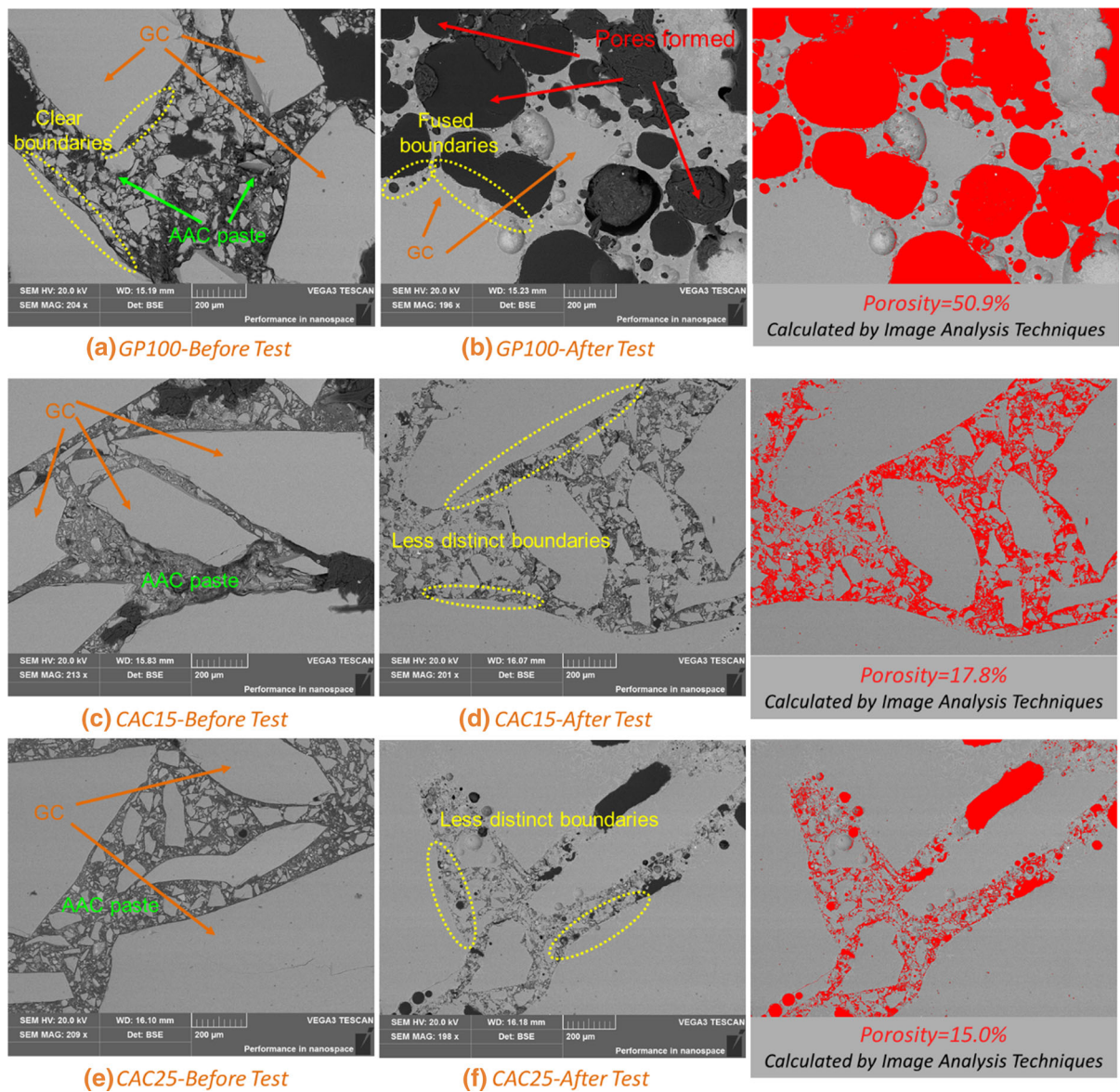
Fig. 6 SEM-BSE images and processed images of CAC incorporated AAC

3.3.2 TGA

The thermal gravimetric analysis test results are shown in Fig. 8.

As observed from the TG curves in Fig. 8, the AAC samples prepared without CAC incorporation showed a total mass loss of about 8.0% after the TG test. While for the AAC mixtures prepared with 15% CAC as the precursor materials, the total mass loss was slightly increased to 9.3%. Increasing the dosage of CAC to 25% resulted in a total mass loss of about 14.0%. One endothermic peak at the temperature range of 250–270 °C can be clearly observed that differentiated the AAC mixtures prepared with/without CAC incorporation, and the peak intensity also increased as the CAC content increased.

The major peak of the DTG curves between 100–200 °C can be attributed to the loss of water from the AAC gels [33]. The CAC15 and CAC25 pastes showed a considerably more intense peak at this range compared to the GP100, which can be explained by the higher amount of AAC gel formed when the
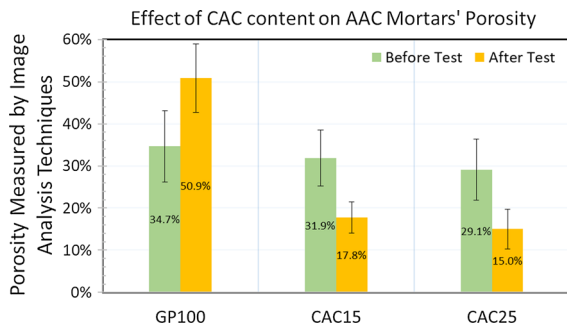
Fig. 7 Porosity of GP-based AAC mortars

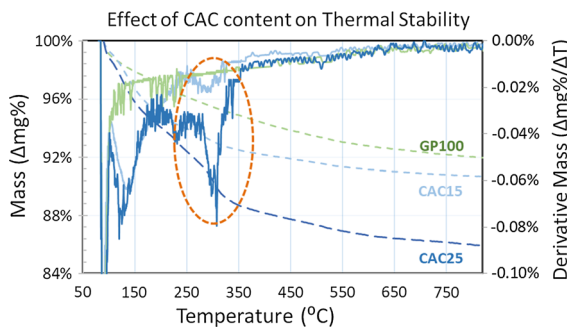Fig. 9 Phase determining of GP-based AAC mortars

Fig. 8 Thermogravimetric analysis of GP-based AAC mortars

more reactive component was used to substitute the less reactive GP.

It was reported that the thermal peak occurred between 250–270 °C could possibly be attributed to the de-hydroxylation of AH_3 [34] or the removal of crystalline water from sodium aluminum silicate hydrate [35].

The dehydration of the reaction products of CAC (sodium aluminum silicate hydrate) in the AAC mixtures implied the probability of increase in porosity. As a result, the expansion pressure of the annealing of the GP can be relieved during the high temperature exposure. A similar mechanism was reported for cementitious materials incorporating polymer fibres [36, 37] due to the generation of voids resulted from the fibre decomposition at elevated temperatures and thus vapor pressure built up can be mitigated.

3.3.3 XRD

The XRD spectra of the samples are shown in Fig. 9.

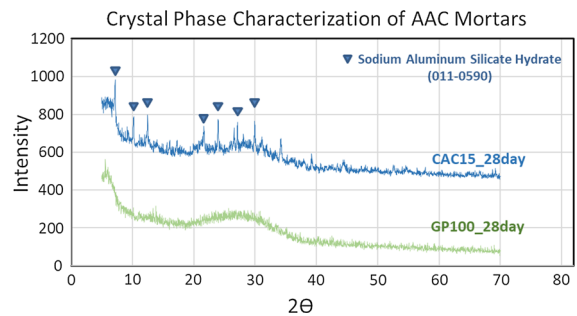For the reference AAC prepared without CAC incorporation, no crystalline phases were detected. However, when 15% CAC was incorporated to partially replace GP as the precursor material, several peaks were detected, among which the most intensive ones appeared at 7.2°, 10.2°, 12.5, 21.7, 24.0°, 27.1° and 29.9° which suggested the presence of sodium aluminum silicate hydrate (011–0590).

As shown in Fig. 8, with increased amount of CAC in the GP based AAC mortar, mass loss occurred in the TG test curve, this can be attributed to the loss of water of crystallization from the sodium aluminum silicate hydrate $((NaAlSiO_4)_{12} \cdot 27H_2O)$ formed. The dehydration process left pores in the structure.

3.3.4 EDX

From the SEM-BSE images, it can be seen from Fig. 6 that before the elevated temperature exposure, the boundaries between the aggregates and the paste were more distinct. While after the test, the boundary became less distinct, which may be attributed to the softening of the glass aggregate. As the major component of the recycled glass materials is SiO_2, elemental characterization was performed via EDX for better understanding the distribution of Si before and after the high temperature exposure. The test was performed at a fixed magnification of 100 times as shown in Fig. 10.

As illustrated by Fig. 10a, c, before the test, the Si concentration in the recycled GC was higher than in the AAC paste part. After the elevated temperature exposure, the difference in Si concentration between the aggregates and the paste became less noticeable as illustrated by Fig. 10b, d which implied some Si had been migrated from the recycled GC to the paste. This process is thought to be pivotal for the residual strength enhancement of the AAC mortar after the high temperature exposure.
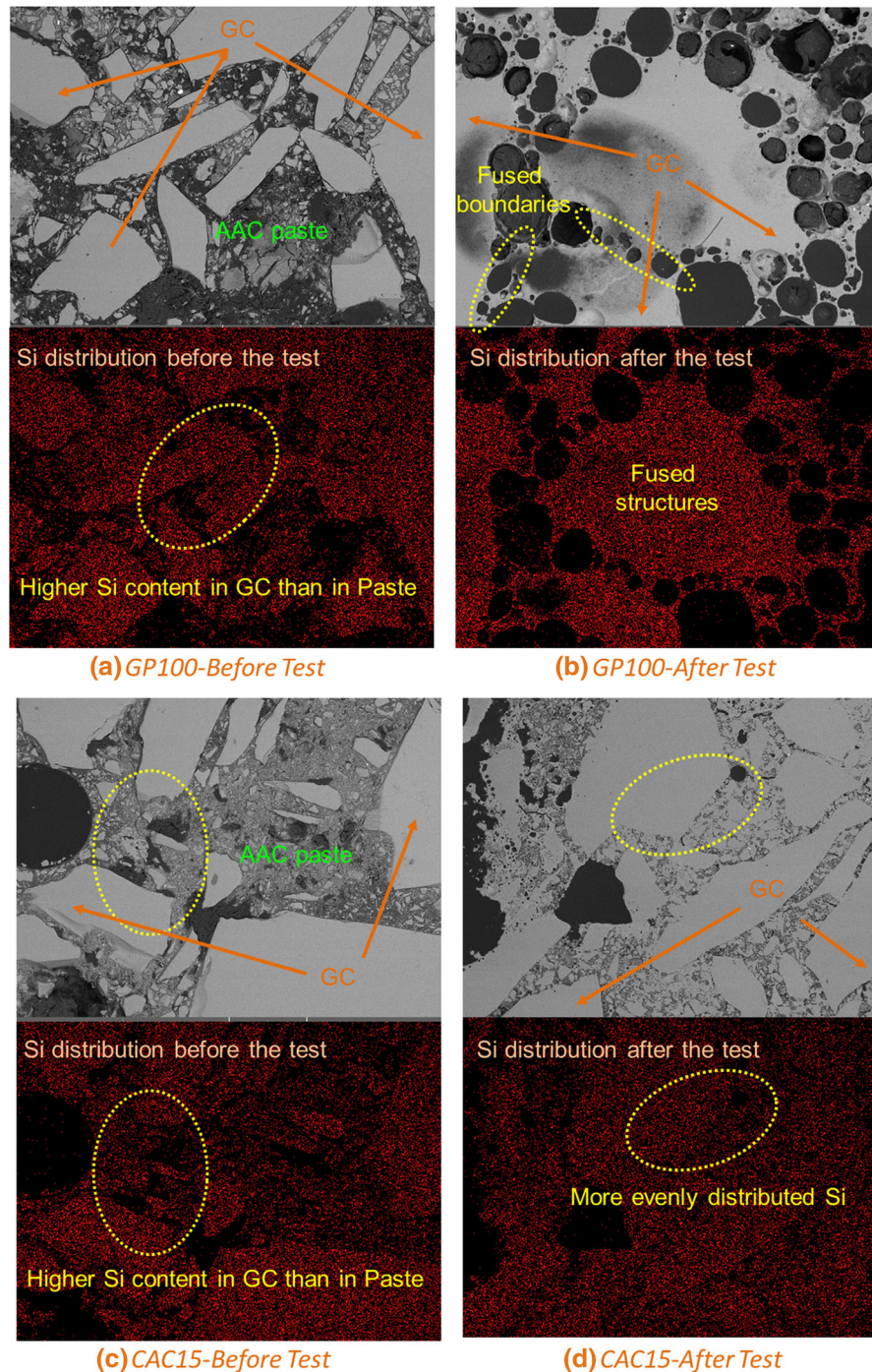
Fig. 10 Elemental characterization—Si Mapping of AAC mortars

The relative concentrations of Si on the AAC paste part of CAC15 mortars before and after the high temperature test were quantified and the results are presented in Fig. 11.

The Si content in the paste of CAC15 was only 15.7% before the elevated temperature exposure test. But after the high temperature exposure, the Si content in the paste was increased to 29.1% (Fig. 11b).
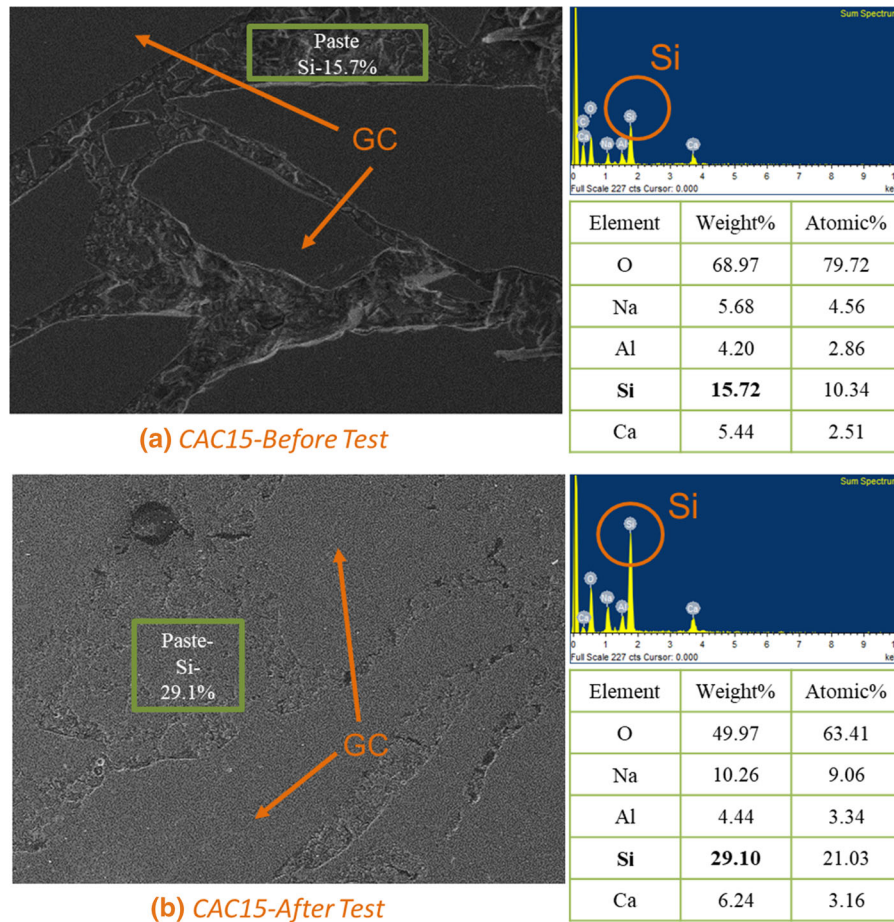
Element	Weight%	Atomic%
O	68.97	79.72
Na	5.68	4.56
Al	4.20	2.86
Si	**15.72**	10.34
Ca	5.44	2.51

(a) *CAC15-Before Test*

Element	Weight%	Atomic%
O	49.97	63.41
Na	10.26	9.06
Al	4.44	3.34
Si	**29.10**	21.03
Ca	6.24	3.16

(b) *CAC15-After Test*

Fig. 11 Elemental characterization—Si quantification for the paste section of CAC15-AAC mortars

A previous study [38] on the performance of CAC under elevated temperature conditions suggested that the addition of silica exhibited positive impact on the hydration products of CAC and thus led to increased compressive strength. The release of Si from the recycled glass as indicated by Fig. 11 may also contributed to the strength gain.

3.3.5 Microhardness evaluation

For the CAC incorporated AAC mortars, the Si release during the elevated temperature exposure (as shown in the EDX characterization results above) led to the formation of a paste with a higher microhardness. For the microhardness evaluation, a set of HVX-1000 digital micro hardness tester was used. The evaluation was conducted on both the paste and the GC aggregate parts for GP100 and CAC15 specimens collected before and after the elevated temperature exposure (800 °C for 2 h). For each sample tested, 40–80 measurements were recorded to calculate the average value and to plot the Vickers hardness distribution profiles.

The distributions of the microhardness values as well as the average microhardness values of each test are summarized in Fig. 12.

Comparing Fig. 12a, b, before the test, the AAC paste of the GP100 mortar and CAC15 mortar had similar Vickers hardness values ranging from 0–100 kg/mm^2. After the test, the GP100 mortar specimen comprised mainly GC and pores as shown in Figs. 6b and 10b, and most of the paste was merged with the GC and was difficult to be identified. Thus, the microhardness distribution curve of the paste of GP100 after the elevated temperature exposure was not plotted. From Fig. 12a it can be seen that the range
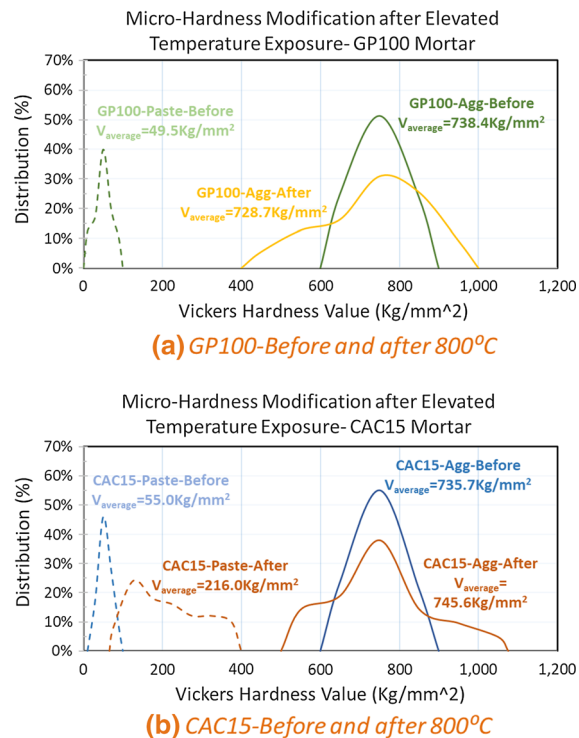
Micro-Hardness Modification after Elevated Temperature Exposure- GP100 Mortar

(a) *GP100-Before and after 800⁰C*

Micro-Hardness Modification after Elevated Temperature Exposure- CAC15 Mortar

(b) *CAC15-Before and after 800⁰C*

Fig. 12 Microhardness characterization

of GC's microhardness extended from 600–900 to 400–1000 K/mm^2. Even so, the presence of a large volume of porosity (over 50%) was detrimental to the residual mechanical properties. Consequently, noticeable strength reduction occurred (about 17% as shown in Fig. 3) after the test.

As demonstrated by Fig. 12b, when CAC was incorporated into the GP dominated AAC mortar, the range of micro-hardness values of the paste was changed from 0–100 to 80–400 kg/mm^2. At the same time, the average micro-hardness value was shifted from 55.0 to 216 kg/mm^2. The significant enhancement is consistent with the strength increment presented by Fig. 3.

3.3.6 FTIR

The FTIR spectra of GP100 and CAC15 are presented in Fig. 13.

As shown in Fig. 13a, b, both GP100 and CAC15 mixtures exhibited a broad intense band around 900–1200 cm^{-1} as a result of alkali activation [39]. The small peak observed at around 1640 cm^{-1} represented the O–H bending from the absorbed

Functional Groups Characterization - GP100

(a) *GP100-Before and after 800⁰C*

Functional Groups Characterization - CAC15

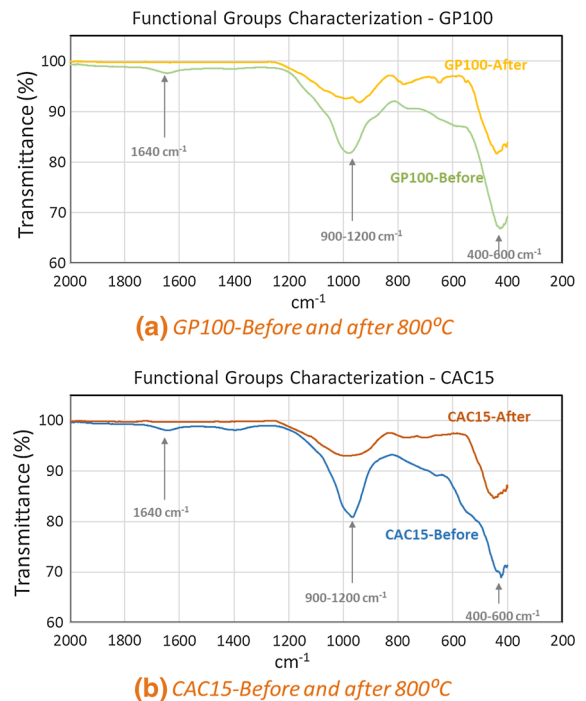**(b)** *CAC15-Before and after 800⁰C*

Fig. 13 Functional groups' characterization by FTIR of GP-based AAC mortars with/without CAC incorporation

atmospheric water [40]. The strong peak at 400–600 cm^{-1} may be due to Si–O–Si and Si–O–Al asymmetric bending [26].

Comparing the FTIR spectra of the samples recorded before and after the high temperature exposure test in Fig. 13a, b, for both GP100 and CAC15, the peaks at 900–1200 cm^{-1} and 400–600 cm^{-1} shrank after the test, which could possibly be attributed to the decomposition of geopolymerization products during the elevated temperature exposure.

For both specimens, the functional groups characterization suggested that no obvious new peak was detected after the elevated temperature exposure, which implied that the strength increment obtained for AAC mortars prepared with 15% to 25% CAC was mainly due to the denser AAC paste generated as a result of the aggregates annealing of the glass materials and pores filling of the partially melted glass.

4 Discussion

In this study, the maximize the recycling of waste glass, recycled GP was used innovatively as the sole

precursor material to prepare the reference AAC mortars while GC was also used as the fine aggregate. However, severe expansion was detected after the elevated temperature resistance test due to the extremely porous structures formed after the high temperature exposure. A novel way of using CAC was developed to mitigate the expansion and strength loss, and the mechanism is illustrated by the diagram below.

As illustrated by Fig. 14, for the GP100 AAC mortar, when the temperature was raised to above 550 °C, the density of glass was reduced, led to volume increment, the original porosity was not enough to accommodate such increment, consequently, mortar expansion occurred. At the same time, GC and paste fused and produced a rigid structure, which inhibited the strain back of glass materials after the temperature cooled down. Therefore, after the test, a fused rigid structure with extremely high porosity was obtained.

While for the CAC incorporated AAC mortars, sodium aluminum silicate hydrate ($(NaAlSiO_4)_{12}$

$\cdot 27H_2O$) was produced as a result of CAC's hydration. When the temperature reached about 250 to 270 °C, the dehydration process took place, which left pores in the structure. As the temperature was further raised to 550 °C, the glass materials (mainly unreacted GP) started to expand, but unlike in GP100 AAC mortar, with CAC's incorporation, the GP induced expansion was accommodated by the pores left after the dehydration process. Therefore, the CAC incorporated AAC mortars exhibited no expansion after the test. At the same time, under elevated temperature conditions, the Si in GC was introduced into the paste and the microhardness of paste was considerably enhanced, which led to the significant strength increment for CAC incorporated AAC mortars after exposure to the elevated temperature condition.

5 Conclusions

Based on the above results and discussion, the following conclusions can be drawn:
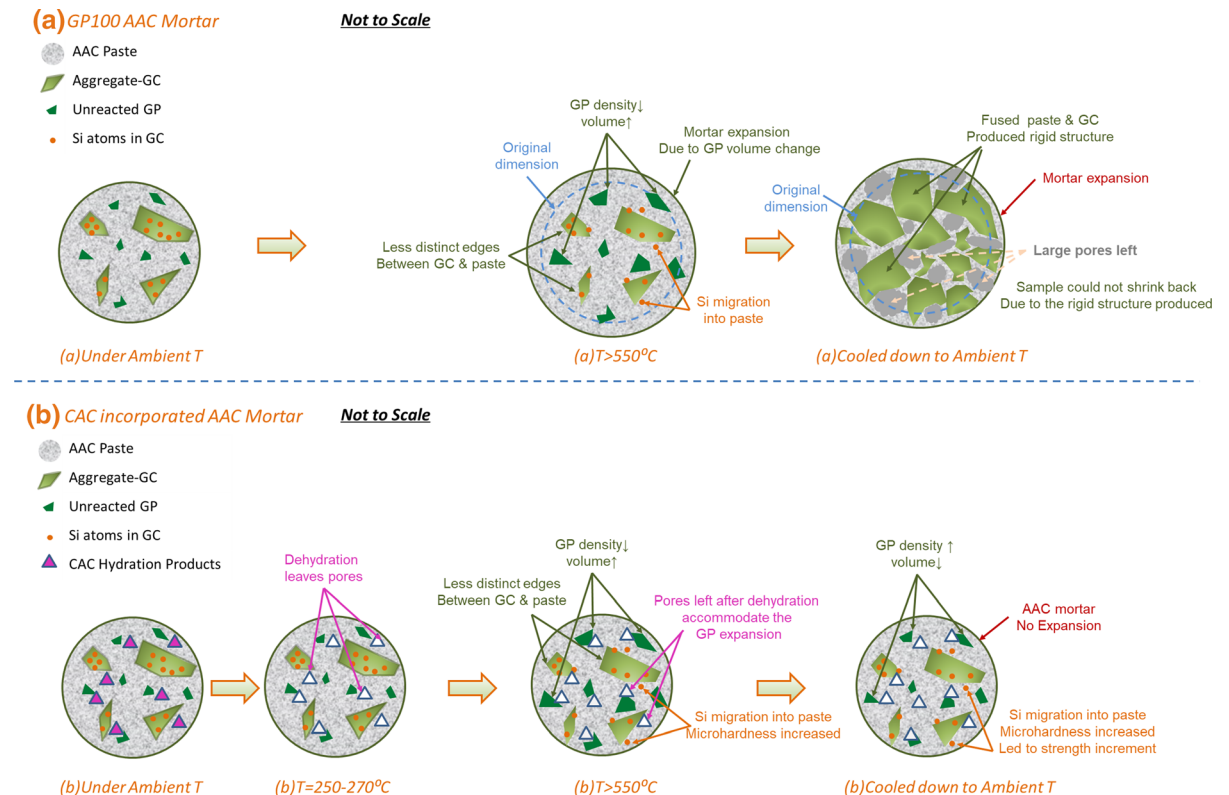

Fig. 14 Illustration of **a** GP100 AAC mortar and **b** CAC incorporated AAC mortars under elevated temperature conditions

1. It is feasible to fabricate recycled glass dominated AAC mortars with superior elevated temperature resistance capacity. A residual strength ratio of over 450% could be attained by appropriate mix proportions;

2. Severe expansion occurred for the GP100 AAC mortars after the elevated temperature exposure and this was attributed to the decreased density of glass materials which led to significant volume increment. The image analysis of the SEM-BSE images indicated that after the high temperature test, GP100 AAC mortar exhibited a porosity of higher than 50%;

3. The incorporation of CAC in the recycled GP dominated AAC mortars modified the pore structures after the high temperature exposure, which can be attributed to the dehydration of CAC reaction products. And the expansion resulted from recycled glass materials softening could be mitigated efficiently, and after the elevated temperature resistance test, negligible dimensional change was observed for the samples prepared with 15% or higher amount of CAC replacing GP as precursor materials;

4. For the CAC15 mortar, the annealing of recycled glass materials introduced Si into the paste and improved the mechanical properties of the AAC gel matrix. However, the GP100 AAC mortar showed significant strength loss after the high temperature exposure due to high thermal instability of the GP;

5. With a carefully designed CAC incorporation, it is feasible to produce recycled glass dominated AAC mortars with higher than 80% of recycled glass materials with good post high temperature performance;

6. On the one hand, the incorporation of small amount CAC into the GP based AAC mortars help to enhance significantly the high temperature resistance capacity of the material, on the other hand, it is feasible to employ the elevated temperature exposure as a pre-treatment measure for CAC-GP based AAC mortars' mechanical properties enhancement.

Declarations

Conflict of interest The authors declare that they have no conflict of interest.

References

1. Kou SC, Poon CS (2009) Properties of self-compacting concrete prepared with recycled glass aggregate. Cem Concr Compos 31(2):107–113. https://doi.org/10.1016/j.cemconcomp.2008.12.002

2. Zhao H, Poon CS, Ling TC (2013) Utilizing recycled cathode ray tube funnel glass sand as river sand replacement in the high-density concrete. J Clean Prod 51:184–190. https://doi.org/10.1016/j.jclepro.2013.01.025

3. Ling TC, Poon CS (2017) Spent fluorescent lamp glass as a substitute for fine aggregate in cement mortar. J Clean Prod 161:646–654. https://doi.org/10.1016/j.jclepro.2017.05.173

4. Pascual AB, Tognonvi MT, Tagnit-Hamou A (2014) Waste glass powder-based alkali-activated mortar. Int J Res Eng Technol 03(25):32–36. https://doi.org/10.15623/ijret.2014.0325006

5. Parghi A, Alam MS (2016) Physical and mechanical properties of cementitious composites containing recycled glass powder (RGP) and styrene butadiene rubber. Constr Build Mater 104:34–43. https://doi.org/10.1016/j.conbuildmat.2015.12.006

6. Tho-in T, Sata V, Boonserm K, Chindaprasirt P (2018) Compressive strength and microstructure analysis of geopolymer paste using waste glass powder and fl y ash. J Clean Prod 172:2892–2898. https://doi.org/10.1016/j.jclepro.2017.11.125

7. Yan R, Yang S, Guo M-Z, Poon CS (2018) Comparative evaluation of fire resistance of partition wall blocks prepared with waste materials. J Clean Prod 182:156–165. https://doi.org/10.1016/J.JCLEPRO.2018.02.020

8. Terro MJ (2006) Properties of concrete made with recycled crushed glass at elevated temperatures. Build Environ 41(5):633–639. https://doi.org/10.1016/j.buildenv.2005.02.018

9. Lu JX, Poon CS (2018) Use of waste glass in alkali activated cement mortar. Constr Build Mater 160:399–407. https://doi.org/10.1016/j.conbuildmat.2017.11.080

10. Lu JX, Poon CS (2018) Improvement of early-age properties for glass-cement mortar by adding nanosilica. Cem Concr Compos 89:18–30. https://doi.org/10.1016/j.cemconcomp.2018.02.010

11. Ramakrishnan K, Pugazhmani G, Sripragadeesh R, Muthu D, Venkatasubramanian C (2017) Experimental study on the mechanical and durability properties of concrete with waste glass powder and ground granulated blast furnace slag as supplementary cementitious materials. Constr Build Mater 156:739–749. https://doi.org/10.1016/j.conbuildmat.2017.08.183

12. Matos AM, Sousa-Coutinho J (2012) Durability of mortar using waste glass powder as cement replacement. Constr

Build Mater 36:205–215. https://doi.org/10.1016/j.conbuildmat.2012.04.027

13. Omran AF, Etienne DM, Harbec D, Tagnit-Hamou A (2017) Long-term performance of glass-powder concrete in large-scale field applications. Constr Build Mater 135:43–58. https://doi.org/10.1016/j.conbuildmat.2016.12.218

14. Pan Z, Tao Z, Murphy T, Wuhrer R (2017) High temperature performance of mortars containing fine glass powders. J Clean Prod 162:16–26. https://doi.org/10.1016/j.jclepro.2017.06.003

15. Zhang S, Keulen A, Arbi K, Ye G (2017) Waste glass as partial mineral precursor in alkali-activated slag/fly ash system. Cem Concr Res 102:29–40. https://doi.org/10.1016/j.cemconres.2017.08.012

16. Liu Y, Shi C, Zhang Z, Li N (2019) An overview on the reuse of waste glasses in alkali-activated materials. Resour Conserv Recycl 144:297–309. https://doi.org/10.1016/j.resconrec.2019.02.007

17. Ali HA, Xuan D, Poon CS (2020) Assessment of long-term reactivity of initially lowly-reactive solid wastes as supplementary cementitious materials (SCMs). Constr Build Mater 232:117192. https://doi.org/10.1016/j.conbuildmat.2019.117192

18. Hussin MW, Bhutta MAR, Azreen M, Ramadhansyah PJ, Mirza J (2015) Performance of blended ash geopolymer concrete at elevated temperatures. Mater Struct Constr 48(3):709–720. https://doi.org/10.1617/s11527-014-0251-5

19. Nasr D, Hossein A, Ghayour H (2018) The influence of curing conditions and alkaline activator concentration on elevated temperature behavior of alkali activated slag (AAS) mortars. Constr Build Mater 190:108–119. https://doi.org/10.1016/j.conbuildmat.2018.09.099

20. Prasittisopin L, Sereewatthanawut I (2019) Dissolution, nucleation, and crystal growth mechanism of calcium aluminate cement. J Sustain Cem Mater 8(3):180–197. https://doi.org/10.1080/21650373.2018.1558132

21. Goergens J, Manninger T, Goetz-Neunhoeffer F (2020) In-situ XRD study of the temperature-dependent early hydration of calcium aluminate cement in a mix with calcite. Cem Concr Res. https://doi.org/10.1016/j.cemconres.2020.106160

22. Palomo A, Grutzeck MW, Blanco MT (1999) Alkali-activated fly ashes A cement for the future. Cement Concr Res 29:1323–1329

23. Duxson P, Provis JL, Lukey GC, van Deventer JSJ (2007) The role of inorganic polymer technology in the development of 'green concrete.' Cem Concr Res 37(12):1590–1597. https://doi.org/10.1016/j.cemconres.2007.08.018

24. Brough AR, Atkinson A (2002) Sodium silicate-based, alkali-activated slag mortars Part I. Strength, hydration and microstructure. Cem Concr Res 32:865–879

25. Arbi K, Palomo A (2013) Alkali-activated blends of calcium aluminate cement and slag / diatomite. Ceram Int 39(8):9237–9245. https://doi.org/10.1016/j.ceramint.2013.05.031

26. Vafaei M, Allahverdi A (2017) High strength geopolymer binder based on waste-glass powder. Adv Powder Technol 28(1):215–222. https://doi.org/10.1016/j.apt.2016.09.034

27. He P, Zhang B, Lu J, Poon CS (2020) A ternary optimization of alkali-activated cement mortars incorporating glass powder, slag and calcium aluminate cement. Constr Build Mater 240:117983. https://doi.org/10.1016/j.conbuildmat.2019.117983

28. Zhang B, He P, Poon CS (2020) Optimizing the use of recycled glass materials in alkali activated cement (AAC) based mortars. J Clean Prod 255:120228. https://doi.org/10.1016/j.jclepro.2020.120228

29. He P, Zhang B, Lu J, Poon CS (2021) Reaction mechanisms of alkali-activated glass powder-ggbs-CAC composites. Cem Concr Compos 122. https://doi.org/10.1016/j.cemconcomp.2021.104143

30. Hasanuzzaman M, Rafferty A, Sajjia M, Olabi A-G (2016) Properties of glass materials. Elsevier Ltd., Amsterdam

31. Zhang B, He P, Poon CS (2020) Improving the high temperature mechanical properties of alkali activated cement (AAC) mortars using recycled glass as aggregates. Cem Concr Compos 112:103654. https://doi.org/10.1016/j.cemconcomp.2020.103654

32. Rukzon S, Chindaprasirt P (2014) Strength and porosity of bagasse ash-based geopolymer mortar. J Appl Sci 14(6):586–591. https://doi.org/10.3923/jas.2014.586.591

33. Li N, Farzadnia N, Shi C (2017) Microstructural changes in alkali-activated slag mortars induced by accelerated carbonation. Cem Concr Res 100(July):214–226. https://doi.org/10.1016/j.cemconres.2017.07.008

34. Fernández-Carrasco L, Rius J, Miravitlles C (2008) Super-critical carbonation of calcium aluminate cement. Cem Concr Res 38(8–9):1033–1037. https://doi.org/10.1016/j.cemconres.2008.02.013

35. Pontikes Y, Nikolopoulos P, Angelopoulos GN (2007) Thermal behaviour of clay mixtures with bauxite residue for the production of heavy-clay ceramics. J Eur Ceram Soc 27(2–3):1645–1649. https://doi.org/10.1016/j.jeurceramsoc.2006.05.067

36. Aydin S, Yazici H, Baradan B (2008) High temperature resistance of normal strength and autoclaved high strength mortars incorporated polypropylene and steel fibers. Constr Build Mater 22(4):504–512. https://doi.org/10.1016/j.conbuildmat.2006.11.003

37. Bernal SA, Bejarano J, Garzón C, Mejía De Gutiérrez R, Delvasto S, Rodríguez ED (2012) Performance of refractory aluminosilicate particle/fiber-reinforced geopolymer composites. Compos Part B Eng 43(4):1919–1928. https://doi.org/10.1016/j.compositesb.2012.02.027

38. Zapata JF, Colorado HA, Gomez MA (2020) Effect of high temperature and additions of silica on the microstructure and properties of calcium aluminate cement pastes. J Sustain Cem Mater 9(6):323–349. https://doi.org/10.1080/21650373.2020.1737593

39. Walkley B et al (2016) Phase evolution of C-(N)-A-S-H/N-A-S-H gel blends investigated via alkali-activation of synthetic calcium aluminosilicate precursors. Cem Concr Res 89:120–135. https://doi.org/10.1016/j.cemconres.2016.08.010

40. Barbosa VFF, MacKenzie KJD, Thaumaturgo C (2000) Synthesis and characterisation of materials based on inorganic polymers of alumina and silica: sodium polysialate polymers. Int J Inorg Mater 2(4):309–317. https://doi.org/10.1016/S1466-6049(00)00041-6